

SpaceOps-2025, ID #250

MAGNETOSPHERIC MULTISCALE MISSION FORMATION FLIGHT DYNAMICS RESULTS: TETRAHEDRON AND STRING OF PEARLS FORMATIONS

Trevor Williams^{a*}, Eric Palmer^a, Neil Ottenstein^b and Vishnu Santhosh^b

^a *Aerospace Engineer, Navigation and Mission Design Branch, NASA Goddard Space Flight Center, Greenbelt, MD 20771.*

^b *Aerospace Engineer, a.i. Solutions, Inc., 4500 Forbes Blvd #300, Lanham, MD 20706.*

* Corresponding Author: Trevor.W.Williams@nasa.gov

Abstract

This paper describes the underlying dynamics of formation flying in a high-eccentricity orbit such as that of the Magnetospheric Multiscale (MMS) mission. The GPS-based method used for MMS navigation is summarized, as well as the procedures that are used to design the maneuvers used to place the spacecraft into a series of relatively small tetrahedron formations and then maintain them there. The details of how to carry out these maneuvers are then discussed. Finally, details are also given of the other types of maneuvers that the MMS spacecraft have had to perform, many of which were driven by the main source of perturbation to the high MMS orbit (with apogee halfway to lunar orbit), namely the gravitational attractions of Sun and Moon.

Keywords: Magnetosphere, Formation Flying, Flight Dynamics

Acronyms

Apogee Raise (AR)
Argument of Perigee (AOP)
Brute Force Monte Carlo (BFMC)
Conjunction Assessment Functional Area (CAFA)
Constellation High Fidelity (CHiFi)
Extended Kalman Filter (EKF)
Flight Dynamics Operations Area (FDOA)
Formation Design Algorithm (FDA)
Formation Initializations (FI)
Formation Maintenance (FM)
Formation Resizes (FRs)
Goddard Enhanced Onboard Navigation System (GEONS)
Goddard Spaceflight Center (GSFC)
Hard-Body Radius (HBR)
Inter-Satellite Range (ISR)
Magnetospheric Multiscale Mission (MMS)
Maneuver Targeting Tool (MTT)
Maneuver Trade Space (MTS)
Mission Operations Center (MOC)
Orbit Determination (OD)
Out-of-Plane (OOP)
Polynomial Chaos Expansion (PCE)
Quality Factor (QF)
Region of Interest (RoI)
Relative Motion Situational Awareness (RMSA)
Right Ascension of the Ascending Node (RAAN)
Resident Space Object (RSO)
Semi-Major Axis (SMA)
Ultra-Stable Oscillator (USO)

1. Introduction

The NASA Magnetospheric Multiscale (MMS) mission is flying four spinning spacecraft (Figure 1) in highly elliptical orbits to study the magnetosphere of the Earth [1]. Launch on an Atlas V 421 occurred from Kennedy Space Center on Mar. 12, 2015, with insertion into a high-eccentricity orbit that was designed to satisfy a complicated set of science and engineering constraints [2]. After roughly 5 months of commissioning, the spacecraft were flown in tetrahedron formations of varying dimensions [3][4] for science data collection. In the first phase of the mission, these measurements were taken on the dayside of the Earth, in a Region of Interest (RoI) (Figure 2) surrounding the apogee of the MMS orbit (radius $12 R_E$). The goal during Phase 1 was to observe the magnetic reconnection events that are expected to occur near the magnetopause, where the solar wind impinges upon the magnetosphere. Measurements during the later Phase 2b, after apogee radius was increased to $25 R_E$ (roughly two fifths of the way to the Moon) [5], were taken in the magnetotail [6], to similarly observe nightside magnetic reconnection events (Figure 2). Taking simultaneous measurements from four spacecraft allows spatial derivatives of the electric and magnetic fields to be determined, allowing all of the terms in Maxwell's equations to be measured. The prime mission was completed successfully in Sept. 2017, and MMS is currently carrying out further science data collection in an extended mission that is expected to continue until at least 2030. Enough fuel remains to fly the spacecraft in formation for this entire period, so enhancing the collection of science data. This is quite different from pre-launch expectations that the spacecraft would perhaps be able to stay in formation for a year or so after the prime mission before fuel ran out.

This paper describes the results that have been obtained to date concerning MMS formation flying. Practical details that must be taken into account in maneuver design include the fact that the spacecraft are spinners with long flexible wire booms: minimizing flexible motion of these booms requires that reorientation of the spacecraft spin axis be kept to a minimum. Orbital maneuvers must therefore be carried out in essentially the nominal science attitude, with spin axis nearly aligned with the Ecliptic normal. These burns make use of a set of monopropellant hydrazine thrusters, two (of thrust 4.5 N) along the spin axis in each sense, and eight (of thrust 18 N) in the spin plane; the latter are pulsed at the spin rate to produce a net Δv . The on-board accelerometer-based Delta-V controller [7] is used to accurately generate a commanded Δv . Navigation makes use of the GSFC-developed Navigator weak-signal GPS-based system [8]: this allows signals to be received even when MMS is flying above the GPS orbits, producing a highly accurate determination of the four MMS orbits. This data is downlinked to the MMS Mission Operations Center (MOC) and used by the MOC Flight Dynamics Operations Area (FDOA) for maneuver design. These commands are then uplinked to the spacecraft and executed autonomously using the controller, with the ground monitoring the burns in real time.

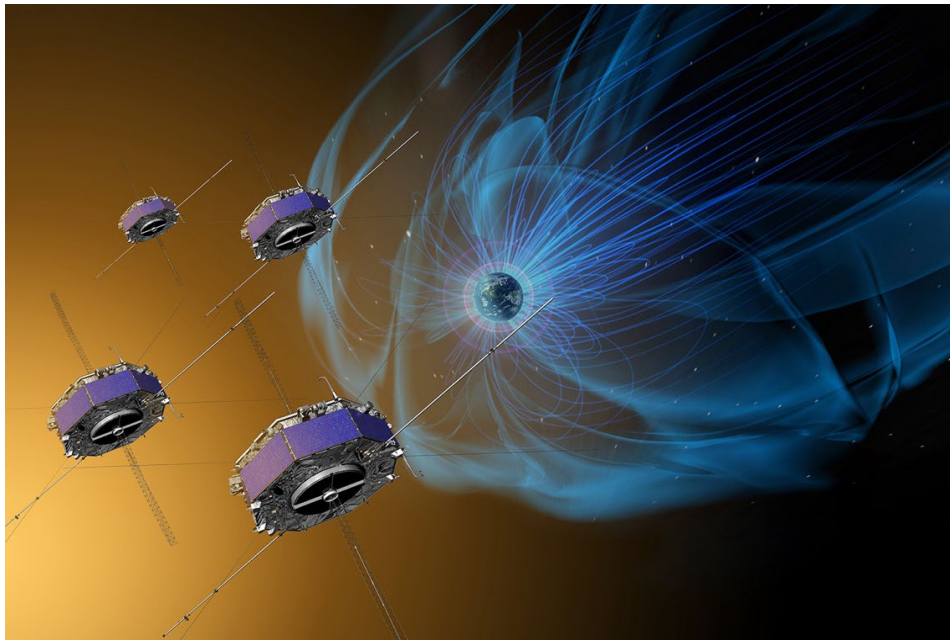


Figure 1. MMS Formation and Notional Magnetosphere

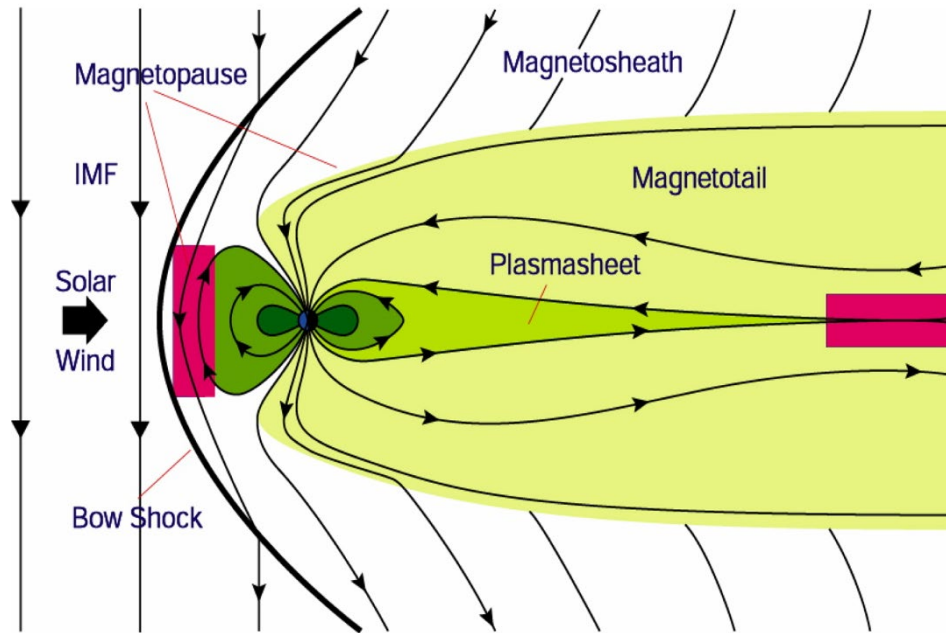


Figure 2. Regions of Phase 1 (left), Phase 2b etc. (right) Science Data Collection

The paper will describe the dynamics of the MMS formation flying problem and show how these drive the design of formation maneuvers. The results that have been obtained over 9 years of flight will be summarized. Another key point is that the MMS orbits currently stretch halfway to the orbit of the Moon, and so experience significant lunisolar gravitational perturbations. One implication of this is that the spacecraft must periodically perform maneuvers to raise perigee and so prevent reentry; another is that the orbits precess slowly relative to the Ecliptic, leading to isolated eclipses that are considerably longer than the spacecraft were designed to survive. Maneuvers had to be designed and performed to mitigate these eclipses. In addition, the reasons why the science team became interested in flying in smaller tetrahedra than originally planned will be summarized, and ways in which this goal was achieved by the flight dynamics team given.

1.1 MMS Launch Window Constraints

The MMS launch was due East from Kennedy Space Center on an Atlas 5 launch vehicle. Initial injection was into a circular parking orbit of altitude 240 km and inclination 28.5 deg. After an appropriate coast period, the Centaur upper stage was reignited to place the spacecraft on an orbit with unchanged perigee altitude and inclination, but with apogee radius $12 R_E$. A series of five maneuvers by the spacecraft over the first two weeks of the mission were then be used to raise perigee radius to $1.2 R_E$, corresponding to an altitude of about 1,276 km.

Although the initial MMS orbit had specified size, shape and perpendicular angle to the Equator, two other parameters were not specified *a priori*: these are the Right Ascension of the Ascending Node (RAAN), Ω_0 , essentially the azimuth of the orbit plane, and the Argument of Perigee (AOP), ω_0 , or the orientation of the line of apsides in the orbit plane. The launch window problem amounts to selecting these two angles so as to ensure that all of the MMS orbital mission constraints are satisfied. Some of these requirements arise from engineering considerations, while others are defined to set the satellites up to collect the desired magnetospheric science. Note that selecting RAAN amounts to fixing the desired time of Atlas launch; selecting AOP corresponds to selecting the coast time between the initial parking orbit injection and the second Centaur burn to place the spacecraft on the highly eccentric MMS orbit.

The MMS mission orbital requirements can be summarized as follows, in the order in which they arise during the mission.

Early mission eclipses - Engineering

No eclipse of duration (defined as that of umbra plus half of penumbra) 1 hr or greater shall occur during the first 14 days of the mission.

Apogee solar longitude at Phase 1 start - Science

Apogee at the end of commissioning must lie near dusk: this corresponds to the start of a sweep by apogee between Earth and Sun, as required for scientific data collection.

Apogee solar latitude at Phases 1a, 1b - Science

In order for the formation to be in position to detect reconnection events during the prime mission dayside passes, it is desired that apogee not be too far out of the ecliptic then. Specifically, the requirement is that the solar latitude of apogee lies in the range ± 20 deg throughout Phase 1a, and ± 25 deg during Phase 2b.

Apogee-raising fuel usage - Engineering

The maneuvers that are used during Phase 2a to raise apogee from $12 R_E$ to $25 R_E$ consume a large fraction of the total MMS fuel capacity: under the most favorable circumstances, they burn around 170 kg out of the total of 410 kg. The particular fuel usage depends on the orbit orientation in a way that will be discussed later: orbit geometries that lead to increased apogee-raising fuel usage are to be avoided.

Eclipse duration (Phase 2b) - Engineering

No eclipse of duration (defined as that of umbra plus half of penumbra) 3.85 hr or greater shall occur at any point during the prime mission or for one year afterwards.

Neutral sheet dwell time - Science

In order to be in position to be able to observe magnetic reconnection events in the magnetotail on the nightside of the Earth, the spacecraft must spend at least 100 hr flying within $0.5 R_E$ of the Fairfield model [2] of the *neutral sheet*, i.e. the surface that separates the northern and southern lobes of the magnetotail. Magnetic reconnection predominantly occurs in the vicinity of the neutral sheet.

A significant difficulty in evaluating these constraints is that many of them apply some considerable time after launch: commissioning takes 4 months, followed by a science mission that is roughly 2 years in duration. Over this interval the orbit is affected strongly by both the oblateness of the Earth, i.e. the J_2 term in the gravity model (because the MMS perigee is relatively low), and by the gravitational attraction of both Sun and Moon (because the MMS apogee is high, particularly during Phase 2b). Consequently, a large part of the effort involved in carrying out an MMS launch window analysis is evaluating the J_2 and lunisolar effects on the orbit, so as to be able to map conditions at any specified point of interest in the mission (e.g. Phase 2a, for apogee-raising) back to the initial launch conditions. This then allows a determination to be made of which RAAN and AOP values at launch lead to the various engineering and science constraints being satisfied.

One further consideration is that the MMS perigee altitude is not allowed to go below 800 km. This is due to the need to reduce the amount of atomic oxygen exposure, which can damage the instruments. Lunisolar perturbations can cause perigee to dip below this threshold, triggering a perigee-raise maneuver. As these use a significant amount of fuel, it is of interest to know how many reboosts are likely to be required for any given launch condition.

Figure 3 encapsulates these constraints in the (RAAN, AOP)-plane as generated by the SWM76 launch window code described in [2]: the various colored shapes indicate the boundaries where each of the constraints is satisfied; the white lozenge then shows where all constraints are satisfied, i.e. the range of acceptable launch conditions. This technique was used to determine the required launch conditions for the actual Mar. 12, 2015 launch date as well as for many other candidate dates (see e.g. Oct. 15, 2014 in Figure 3), so specifying the range of those that were acceptable for launch.

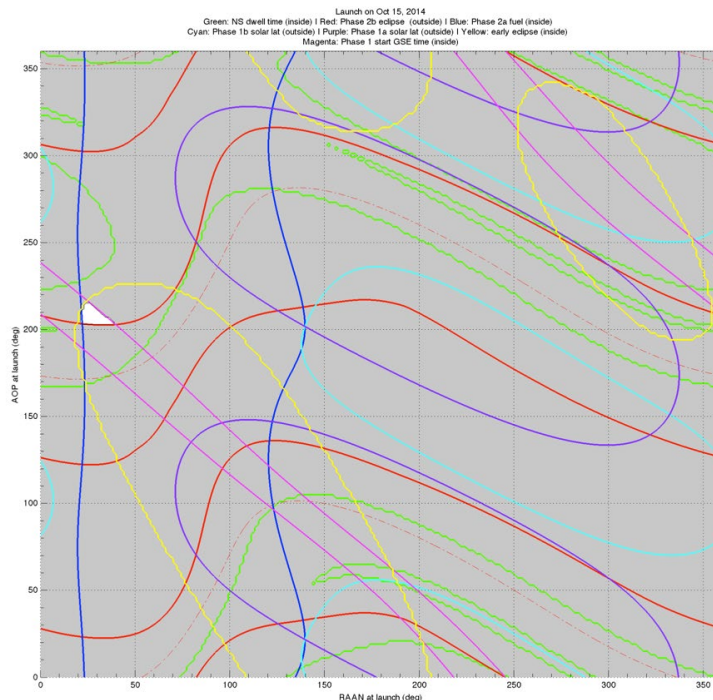


Figure 3. Launch Window Scan, Candidate Oct. 15, 2014 Launch Date

1.2 MMS Formation Flying Background

In order to collect the science data that is required in order to study magnetic reconnection, the MMS spacecraft must form a tetrahedron formation (so spanning all three axes) while transiting the science RoI of the orbit. This region is an extended arc centered on apogee where the radius of the orbit is in the range where reconnection is expected to occur: for the MMS Phase 1 orbit this is 9 Earth radii (R_E) or greater, switching to 15 R_E or greater for Phase 2b and the extended mission. It should be noted that the orientation of the tetrahedron is not specified: any orientation will give the spread across each of the three axes that is required for science.

In order for the formation to persist over multiple orbits (referred to below as revs), it is necessary for the spacecraft to take up essentially the same relative positions from one rev to the next. If this is to occur, the four MMS orbits must have essentially equal periods. Since period is directly related to semi-major axis (SMA), the key is to have the SMAs of the four orbits be closely matched: any differences will lead to drift rates (which can be either expanding or closing) between the spacecraft. Once the accumulated drift is sufficiently large, the tetrahedron will be distorted enough that it is no longer suitable for science data collection: maneuvers must then be performed to reestablish a high-quality formation.

Since the MMS orbit is highly eccentric (eccentricity 0.818 for Phase 1, 0.908 for Phase 2b, and around 0.92 throughout the extended mission), the behavior of the formation when traveling from apogee to perigee and back is quite complicated. Consider the along-track separation between any pair of spacecraft: this is created by setting up the appropriate difference in phasing between the satellites. For instance, suppose that an along-track spacing of 18 km were required at apogee during Phase 1: since orbital speed at apogee is approximately 0.9 km/s, this will be achieved by having one spacecraft fly 20 s ahead of the other. But the orbital speed at perigee is around 9 km/s: this same lead time will therefore result in an along-track spacing of 180 km at perigee, a tenfold increase. This “breathing mode” around the orbit implies that along-track separation in the RoI will be at its minimum at apogee, increasing somewhat in the vicinity of RoI entry and exit.

The out-of-plane (OOP) relative motion is quite different. To have a specified (and maximal) OOP spacing at apogee, the common (or node) points of the corresponding pair of MMS orbits should occur at true anomalies in the vicinity of 90 deg and 270 deg. As a result of this geometry, and since apogee radius is 10 times as large as perigee

radius, the OOP spacing will be roughly 10 times greater at apogee than at perigee. Furthermore, the sign of the relative displacement changes going from apogee to perigee: the spacecraft swap sides. Consequently, the most likely places for close approaches to occur between a pair of MMSs are at true anomalies around 90 deg or 270 deg. Care is taken in the formation maneuver design process to ensure that this does not occur.

Finally, since the orbits must have the same SMAs, any radial separation between these spacecraft at apogee must be set up by introducing a small difference in eccentricity, e : one orbit will therefore have apogee radius above the other, and perigee radius below it. The radial separation therefore changes sign when going from apogee to perigee, but the magnitudes at perigee and apogee are equal.

As a result of these effects, a tetrahedron that is suitable for science will approximate a regular tetrahedron throughout the RoI, although being slightly “squashed” at apogee. At perigee, it will be extremely elongated, no longer even remotely resembling a regular tetrahedron, and will have “flipped” in the OOP and radial directions. This complicated motion to some extent approximates a tumble, with superimposed elongation and then recompression as the formation passes from apogee to perigee and back, while the same behavior is repeated from one rev to the next. Figure 4 shows the corresponding evolution in inter-satellite ranges between the 6 MMS pairs over the orbit for one of these formations. The large spikes in inter-satellite range (ISR) caused by the along-track elongation of the formation around perigee can clearly be seen.

The Quality Factor (QF) is a dimensionless parameter, lying between 0 and 1, that quantifies how close a formation is to a regular tetrahedron of the desired size: the closer to 1, the more suitable the formation. Figure 5 shows an example of the QF over several revs, from one formation to the next: the characteristic “double hump” evident in this plot is a result of the fact, discussed previously, that the formation is somewhat compressed at apogee, leading to a lower QF value at apogee itself than shortly before or after it. It can be seen that one of the two peaks gradually builds up from one rev to the next, making the QF plot increasingly unsymmetrical: this is typical of the effect of inter-satellite drift, and eventually leads to the need to perform a set of formation maneuvers to initialize a new tetrahedron. In addition to the instantaneous QF, Figure 5 also displays the mean quality factor per RoI (\bar{Q}), as well as the percent RoI time with QF above 0.7 (T_q). Both values are used as single value assessments of the formation quality over an entire rev. Definitive values for these properties are used as part of science data evaluation and predicted values for these properties are considered when determining when an extra formation maneuver may need to be performed in order to maintain a formation with sufficient quality for science purposes.

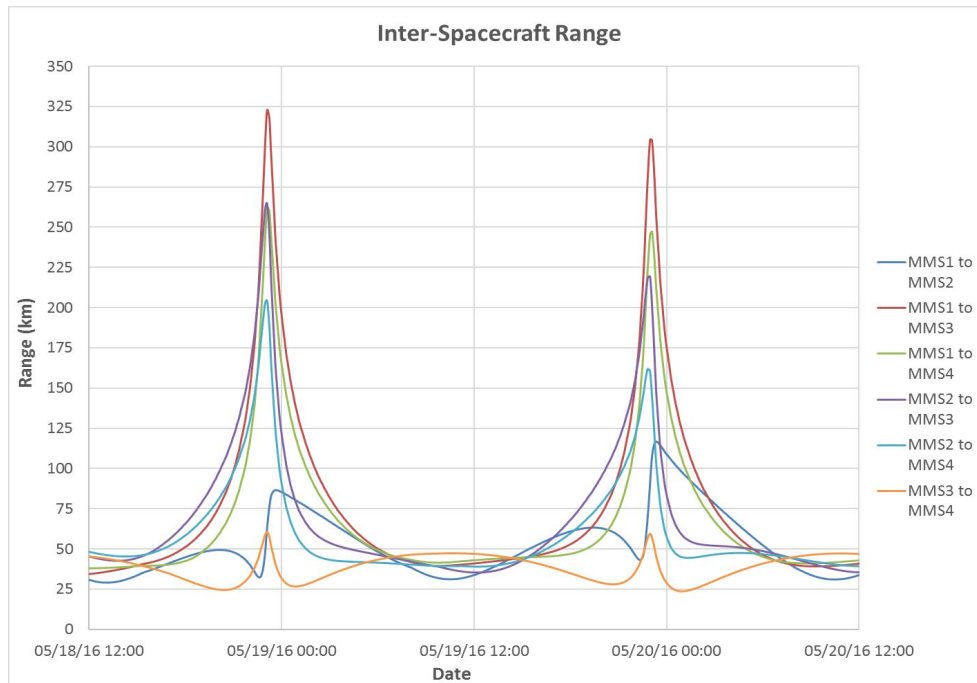


Figure 4. Six Inter-Satellite Ranges Over an Entire Orbit, 40 km Formation

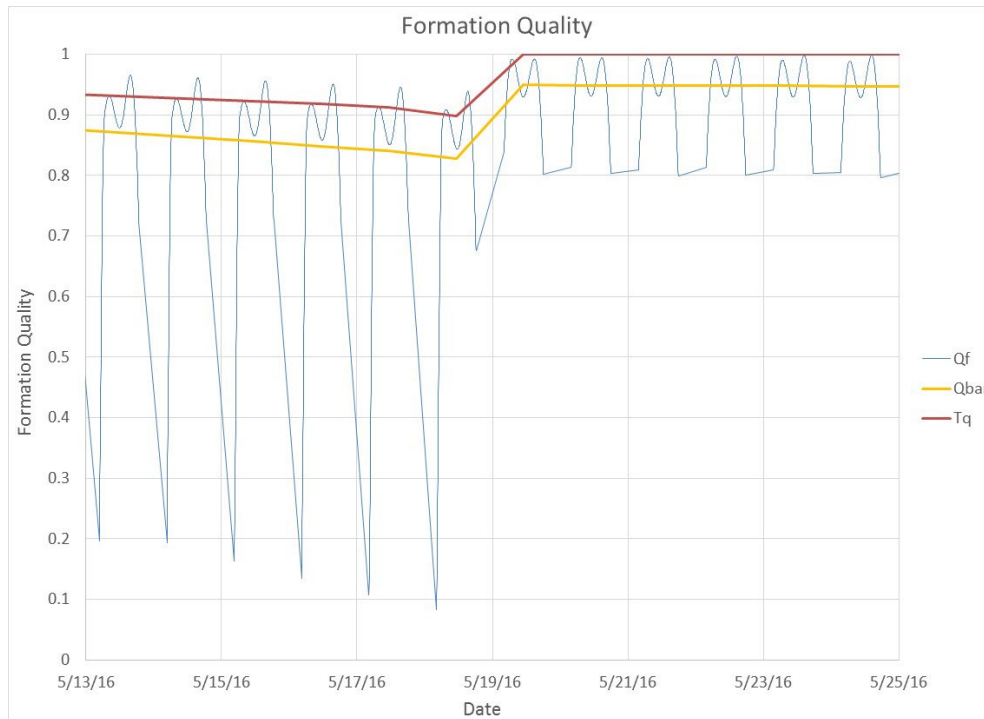


Figure 5. Quality Factor Evolution, Two 40 km Formations

Figure 6 confirms the previous statement that the SMAs of the MMS spacecraft must be essentially equal for any viable formation. The plot covers a complete set of Formation Maintenance (FM) maneuvers: it can be seen that the final SMAs are indeed very nearly equal, as indeed were the SMAs before the maneuvers. Since the reference spacecraft does not maneuver, and so has a constant SMA (modulo orbital perturbations) across the FM maneuver set, it can be seen that the SMA change that is produced by the second burn of each maneuvering spacecraft must be very nearly equal and opposite to that produced by its first burn.

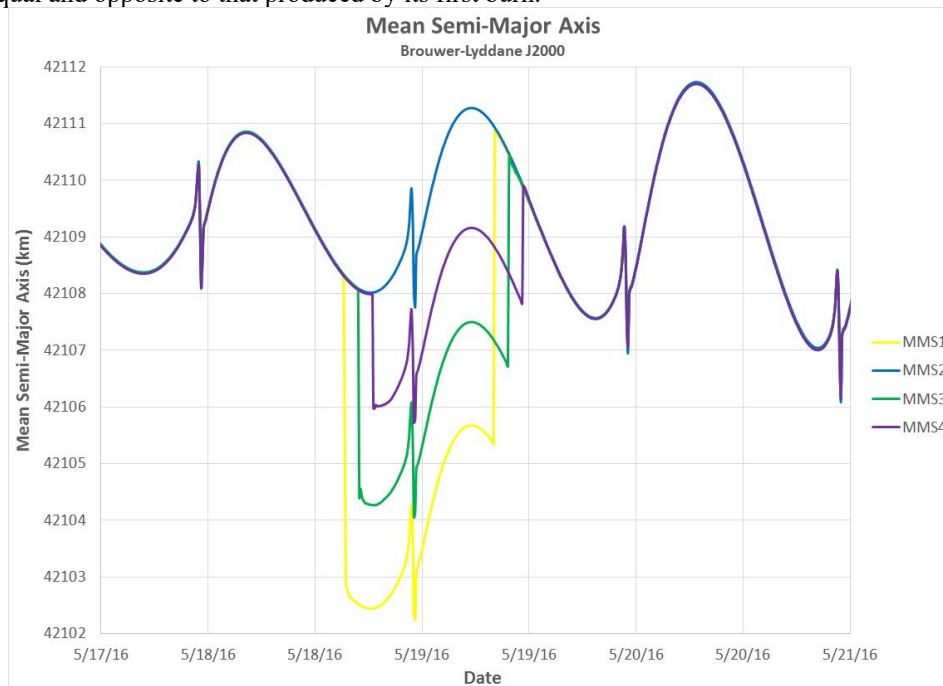


Figure 6. SMAs of the Four Spacecraft Over Set of FM Maneuvers

2. MMS Maneuvers and Results

2.1 Formation Maneuver Design Process

The MMS formation maneuver sequence is based on shifting the spacecraft into a fresh formation arrangement. To do so, one of the spacecraft is selected as a reference and does not performing any ΔV maneuvers. The other three spacecraft perform ΔV maneuvers so as to position themselves into desired orbits relative to the reference spacecraft, such that the four create a tetrahedron while within the RoI. Each of the non-reference spacecraft carries out two burns: the first (FM1) on the orbit flank after apogee, and the second (FM2) in the vicinity of the subsequent apogee. This can be considered as a rendezvous pair: the first burn transfers the spacecraft from its position in the existing formation to its desired location in the new formation; the second burn then modifies its velocity so as to ensure that it continues to track the new formation geometry.

The MMS Formation Design Algorithm (FDA) (see [9] for further details) designs these maneuvers by optimizing them in order to maximize the QF. Given the previous discussion on the evolution of the formation geometry throughout the RoI, it is necessary to allow a range of sizes throughout the RoI: for instance, for a 10 km formation the instantaneous mean sidelength is deemed acceptable if lying in the range 6 to 18 km. The FDA performs a numerical optimization of the QF, subject to two key constraints: firstly, as previously noted, in order for the formation to persist, the SMAs of the four orbits must be matched; secondly, in order to ensure safety of the spacecraft, no ISR is allowed to go below a specified lower limit at any point on the orbit.

The orbit determination data that is used as input to the FDA is produced by the on-board Goddard Enhanced Onboard Navigation System (GEONS) [8]. GEONS estimates the spacecraft's position, velocity, clock bias, clock bias rate, and clock bias acceleration using an Extended Kalman Filter (EKF) coupled with a high-fidelity dynamics model to process GPS L1 pseudorange measurements referenced to the Ultra-Stable Oscillator (USO) clock. The Navigator's weak signal acquisition capability allows the receiver to acquire and track GPS signals well above the GPS constellation and deliver highly accurate navigation solutions. The key MMS on-board orbit determination (OD) requirements were designed to ensure that the FDOA team would be able to safely and accurately maintain the range of nominal formation sizes throughout the mission. Given the extreme importance of SMA for evaluating formation persistence, the most critical requirement from GEONS is to determine SMA accurately. This is best evaluated from state data obtained after each perigee passage, when the MMS orbit passes below the GPS constellation: GEONS then has access to main lobe signals from typically 12 GPS satellites.

The MMS closed-loop Delta-V controller has greatly exceeded its specified performance (see [4]), but can yield comparatively large errors in both magnitude and direction for the smallest maneuver sizes. Consequently, a rule of thumb that was developed was that no burn smaller than 0.05 m/s would be deemed acceptable: this is easily met for the maneuvers to set up larger formations, but can be challenging for the FDA for smaller ones, e.g. 7 km in Phase 1 or 20 km in Phase 2b and the extended mission.

Further details of the MMS formation maneuver design and execution process are given in [4].

2.2 Formation Flying Results to Date

The MMS spacecraft have performed a total of 170 maneuvers consisting of 850 burns as of Feb 18, 2025 the bulk of these make up formation initialization, resize or maintenance sets, but also included are apogee-raises, perigee-raises and slews. The spacecraft each initially held 412 kg of fuel; the current values for their fuel remaining (from bookkeeping) are 95.6-98.1 kg: see Figure 7. The largest decreases in fuel correspond to the Phase 2a apogee-raise campaign. Also noticeable are the effects of the initial perigee-raise maneuvers that each spacecraft had to carry out shortly after launch, and the second set of apogee-raises in early 2019. The largest remaining maneuvers are further perigee-raises, Formation Initializations (FI) and the various Formation Resizes (FRs). An attempt has been made to balance the fuel remaining on each spacecraft by judicious selection of the reference spacecraft for each set of formation maneuvers: it can be seen that this goal has been closely achieved.

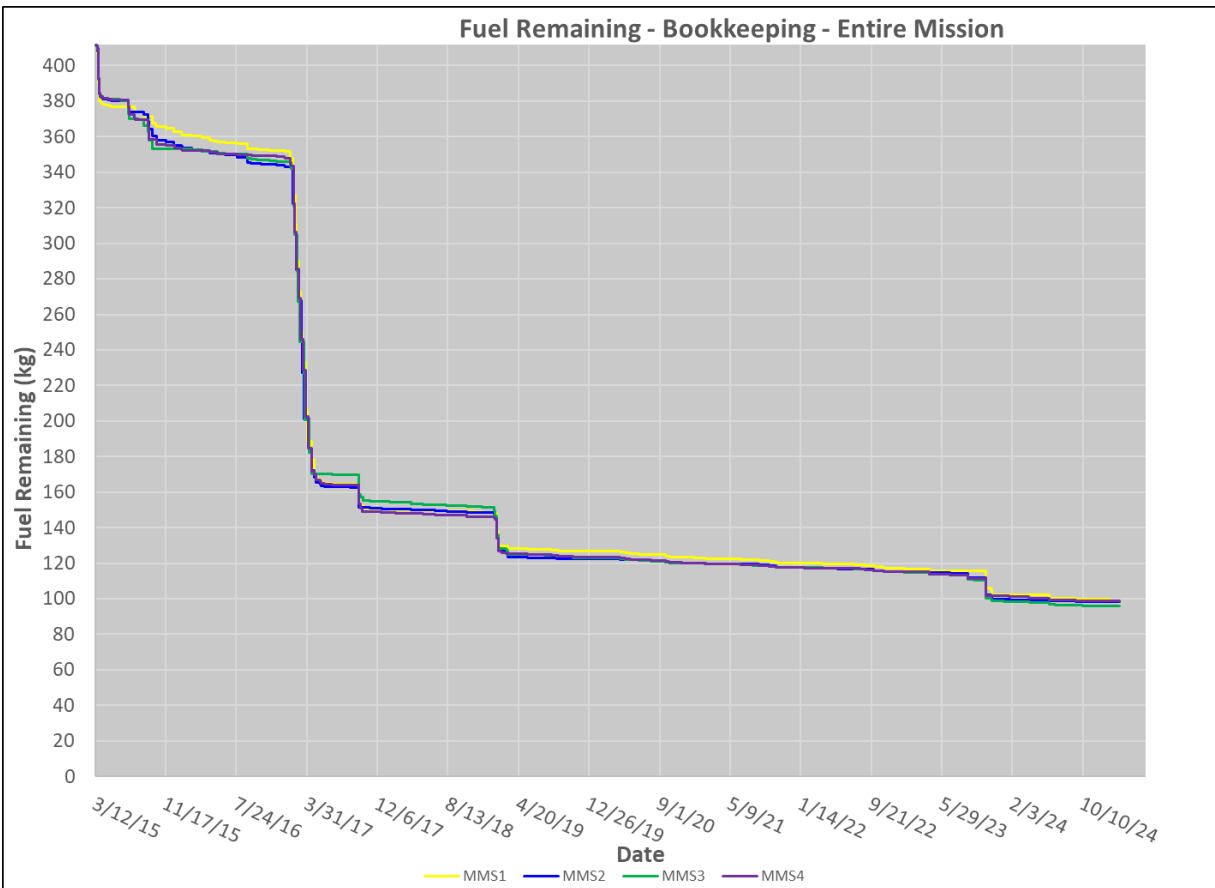


Figure 7. Fuel Remaining per Spacecraft

Maintaining a given formation size is relatively inexpensive in terms of fuel: excluding the initial relatively large resize maneuvers, the average consumption rate is around 2 kg/year per MMS in the extended mission. This economy is partly a result of the relatively small formations that are being flown, and partly a consequence of the slower relative motion in the Region of Interest that surrounds apogee in the current high orbit. In addition, the superior performance of the MMS closed-loop DV controller and the Navigator/GEONS system gives smaller than specified maneuver execution and navigation errors: since such errors typically drive how long the formation will persist before a new set of maneuvers must be performed, this leads to only infrequent maneuvers (typically around quarterly), and so low fuel consumption. Combining this with the efficiency of the apogee-raise maneuvers (by far the largest deterministic fuel cost of the entire mission) leads to the fact that MMS will be able to continue flying in formation until at least 2030.

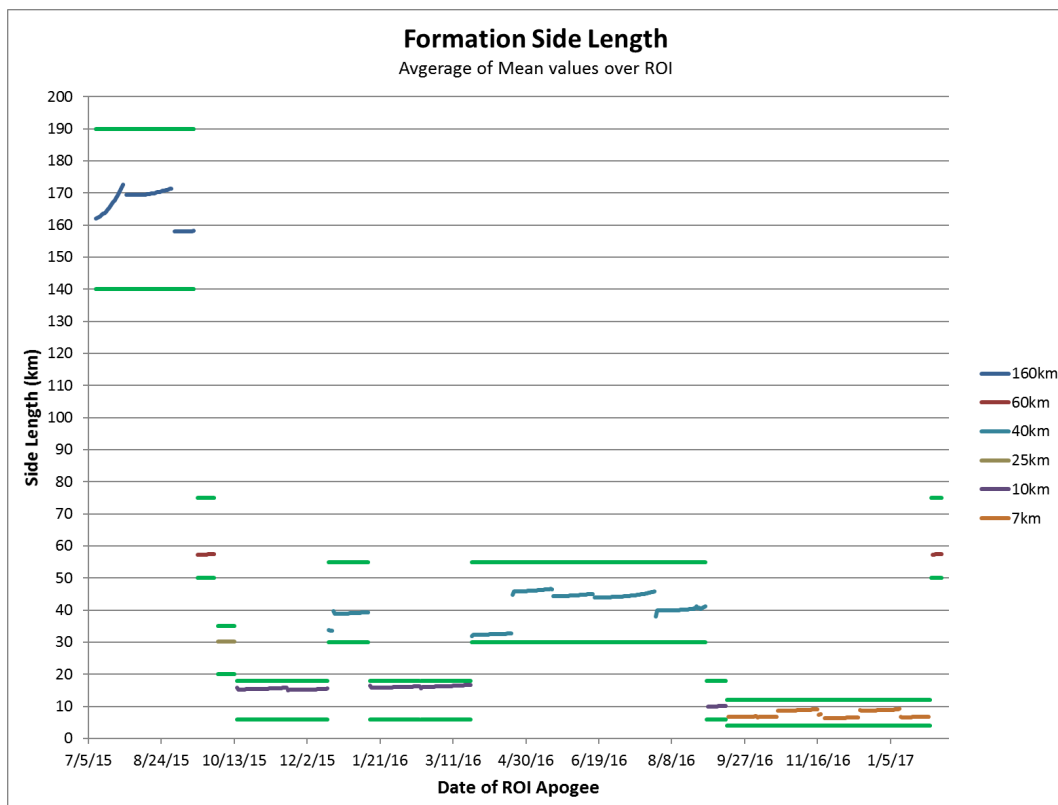


Figure 8. Evolution of Mean Sidelength Averaged Over RoI, Launch to Phase 2a

For each formation flown in Phase 1 (the plot is restricted to this phase, to improve legibility), Figure 8 shows the average over the RoI of the mean of the six sidelengths: this gives a single value for each rev. The green horizontal lines are the bounds on mean sidelength that are allowed from the definition of the QF for a target scale size. These can be thought of as the range of formation sizes that are acceptably close to the target from the point of view of science data collection. Each of the flown formations satisfied this size requirement for extended periods, typically around 3-4 weeks. An exception to this is the early formation resizes to 25 km and then 10 km: these were scheduled to occur every 2 weeks, regardless of whether the QF would have allowed longer flight at the preceding size.

It can be seen that the 10 km formations in late 2015 and early 2016 actually had an averaged mean sidelength of around 15 km; likewise, the preceding 25 km formation was closer to 30 km. The reason for this was the close approach safety limits that are taken into account when designing formations: these tend to bias smaller formations to the upper portion of their allowable size range. While such formations clearly satisfy the science size bounds, it was desirable to try to design formations closer to the target size. This was achieved by using a much tighter set of acceptable size limits when running the FDA to generate a new formation; the original science size limits are still used when evaluating the QF to determine when maneuvers are required later to reset the formation. This technique can be seen in Figure 8 to allow a “true” 10 km formation to be generated in Sept. 2016, followed by a set of 7 km formations that were flown throughout Phase 1b in late 2016/early 2017.

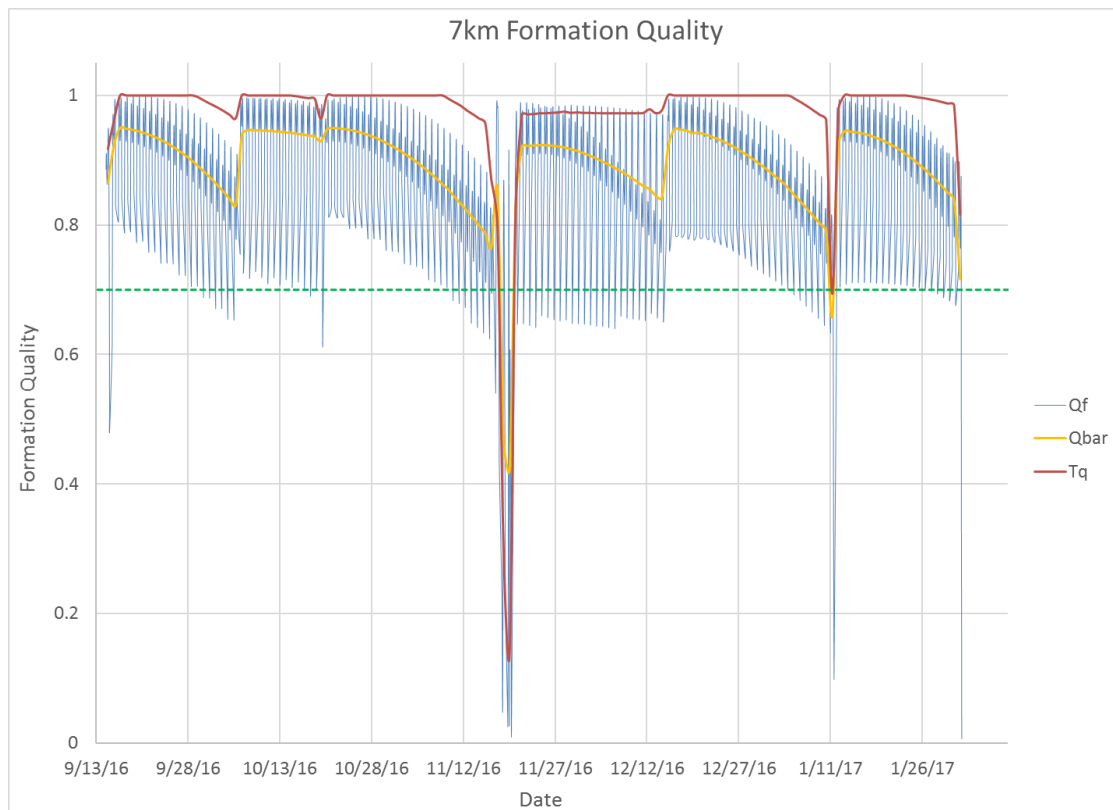


Figure 9. Evolution of Formation Quality Factor, Phase 1b

Figure 9 shows the evolution of formation QF over Phase 1b. If a set of formation maneuvers is triggered because the formation has degraded to the point where its QF is no longer acceptable, it will occur before the quantity T_q hits the 0.7 limit. It can be seen that this threshold was hardly ever reached during Phase 1b: this is a result of the fact that most formation maneuvers were triggered not as a result of QF degradation, but rather in order to prevent an uncomfortably close pass between two spacecraft. The exception is the downward spike in Nov. 2016: this followed an event where MMS3 had a missed burn, leading to it shifting considerably away from its desired position in the formation.

2.3 Trim Burns

It has often been found while flying at small formation sizes that one particular spacecraft pair drifts slowly towards each other. The resulting danger of a conjunction then required that an FM maneuver set be carried out in order to “reset” the formation. In several cases, this had to be done earlier than originally planned, which led to disruption to science collection (since FM maneuvers occur in the science RoI) and additional fuel use. The underlying reason for this inter-satellite drift is that execution errors in the preceding FM set led to the semi-major axes of the drifting spacecraft being somewhat different, leading to different orbital periods and hence a slow drift rate.

The trim burn was designed after launch, during the Phase 1b small formation flight period, in order to avoid this difficulty. This is a single burn by one of the spacecraft in the drifting pair, and is designed to reduce (ideally, null) the SMA difference between it and the other drifting MMS. Burns to change SMA are typically applied along the orbital velocity vector, as this is the most efficient direction. However, the SMA difference to be corrected in the trim case was typically small, on the order of 10 m, and the required burn size to correct this with a burn along the velocity would be too small to be feasible. In particular, it would be well below the 0.05 m/s maneuver lower limit imposed when using the MMS closed-loop Delta-v controller. Consequently, the trim burn uses the MMS open-loop “Checkout Mode” to apply a small Δv along the spin axis of the spacecraft, using a pair of 4.5 N (1 lbf) axial thrusters. Rather than commanding a desired Δv vector in Checkout Mode, the input that is uploaded to the spacecraft is the desired burn duration of the thrusters.

A limitation of Checkout Mode is that it does not make use of the rotational phasing of the spacecraft. For this reason, this mode cannot be used to apply a Δv with a component along a specified inertial direction in the MMS spin plane. This led to the decision to thrust only along the spin axis. So long as this vector is not perpendicular to the orbital velocity vector (which only occurs twice per orbit), there is a component of Δv along the orbital velocity vector, and consequently the desired small change in SMA can be produced.

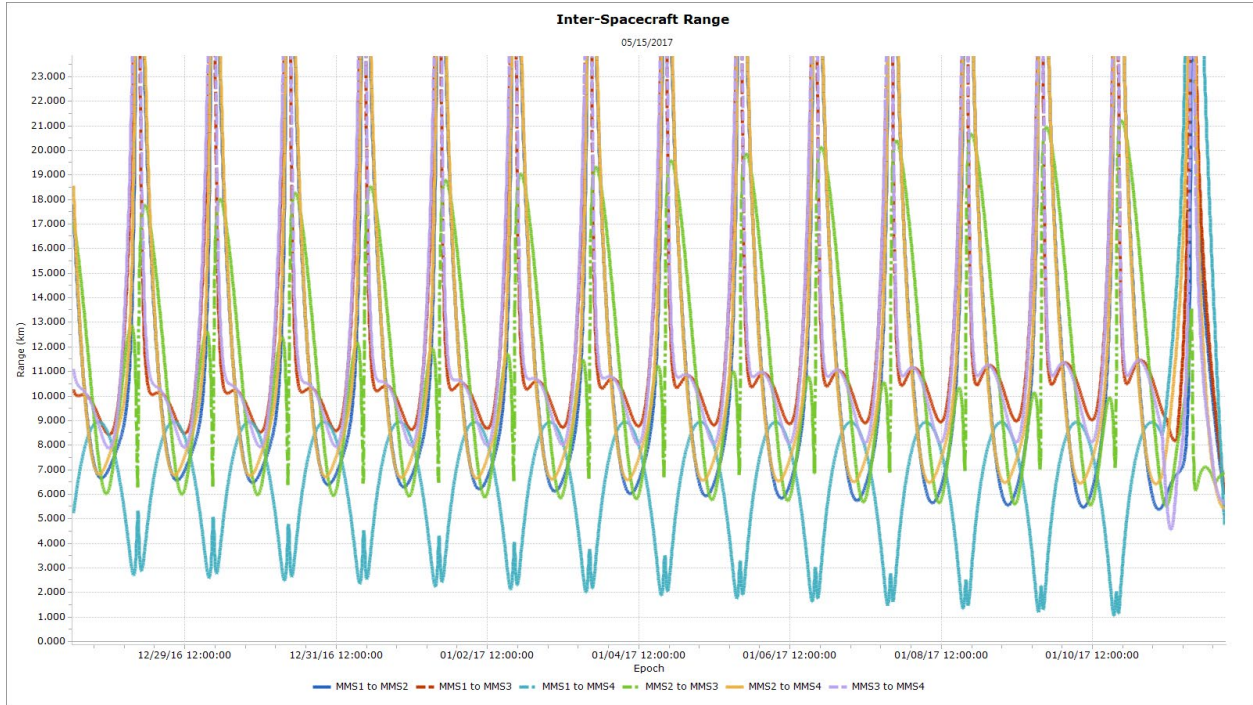


Figure 10. Evolution of ISRs, no MMS1 Trim

Following design, development and testing, the trim burn was ready for application during the latter portion of Phase 1b. The opportunity arose following an FM set of maneuvers that took place in mid-Dec. 2016. Figure 10 shows the ISR between the 6 MMS pairs: it can be seen that the MMS1/MMS4 pair has a closing drift rate, which normally would have required bringing forward the next formation maintenance maneuvers. Instead, applying a trim burn on Dec. 28 nulled this drift and demonstrated the new type of maneuver. The 0.8 s trim proved very accurate at nulling the 10 m SMA difference between MMS1 and MMS4, and hence their closing rate. This accuracy confirms that the actual force applied by the axial thrusters was very close to the predicted value: in this sense, the trim burn also functioned as a calibration maneuver. Figure 11 then gives the resulting post-trim ISRs: it can be seen that there is now an essentially zero drift rate between MMS1 and MMS4.

A final point concerning the trim burn is that the total fuel consumption was extremely modest: approximately 2.7 grams, as opposed to on the order of 0.2 kg per spacecraft for a typical FM set. In addition, performing a single burn on one spacecraft, rather than two burns on each of three as in a regular FM set, is a considerable operational simplification. It has proved to be a useful tool for flight in small formations, for instance the 20 km dayside tetrahedra in the extended mission.

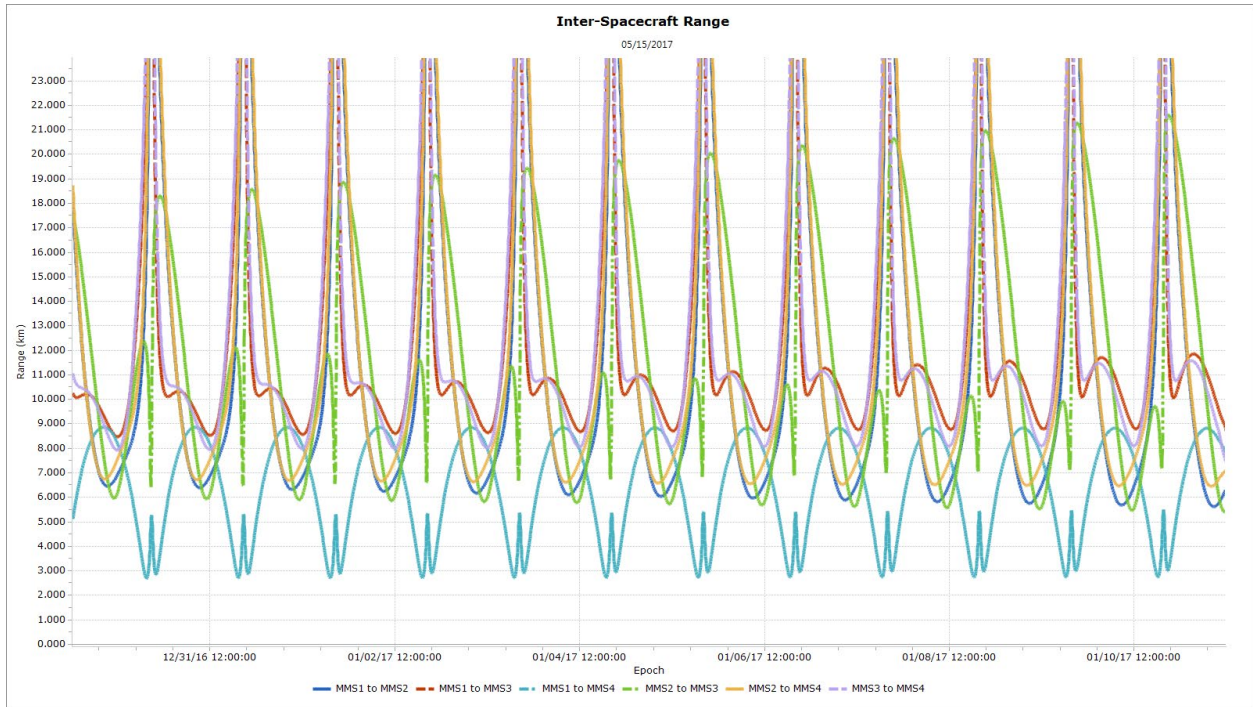


Figure 11. Evolution of ISRs After MMS1 Trim

3. MMS Conjunction Assessment Methods and Tools

For spacecraft that fly in such close proximity to each other, conjunction assessment is clearly an important consideration for MMS. By and large, conjunctions are “designed out” by imposing a minimum separation threshold when designing formation maneuvers. However, techniques have been developed in case a conjunction between two MMSs is predicted, for instance as a result of maneuver execution errors or a missed burn. In addition, conjunctions between an MMS and some resident space objects are also possible, although extremely uncommon as a result of the high perigee of the MMS orbit.

In one key test, nominal MMS spacecraft states and a distribution of modeled maneuver execution errors are used to generate sample trajectories for the Maneuver Targeting Tool (MTT). In this process, 100 (or sometimes 250) sample trajectories of the MMS spacecraft are propagated using a low fidelity model which includes simulations of a formation maneuver set. Such a set consists of two maneuvers by each of three spacecraft; the fourth MMS takes the role of non-maneuvering reference. The results are then analyzed in order to determine the overall feasibility and efficacy of the maneuver design. A failing grade from this inspection results in the rejection of this possible set of formation maneuvers, while a pass moves on to the next step, in which the Constellation High Fidelity (CHiFi) tool is run in a Monte Carlo mode known as Casino to propagate an ensemble derived from the designed initial state, maneuver execution errors, and navigation errors, to the time of the first maneuver. At this point, the first and second moments of the quantities of interest are used to infer a Gaussian distribution for the state of each spacecraft. With these assumptions and moments, random variables with appropriate statistics are then considered in the Brute Force Monte Carlo (BFMC) scheme: the standard MMS implementation considers 75,000 cases. At the planned time of the second maneuver, the process is repeated.

If any interval with a non-zero number of hits is detected, random variables are again generated from the Gaussian assumptions derived at the end of the Casino runs and act as training samples for the calculation of Polynomial Chaos Expansion (PCE)-based collision probabilities at each time step of the aforementioned interval, as [11] describes. Finally, once the maneuvers have been performed and post-maneuver navigation solutions are available from the spacecraft, a process of calculating the probability of collision is carried out after each perigee pass as part of the CAFA tool suite (see below), in a manner essentially similar to the BFMC/PCE process just described.

One area where these conjunction tests has proved important is that of determining the smallest safe formation size. Prior to launch, the minimum size was decided on as 10 km in Phase 1 and 30 km in Phase 2b. However, after examining data generated in flight, the science team determined that, in order to study the electron diffusion region in detail, a formation size of 5 km would be ideal for Phase 1. Using MTT results, the flight dynamics team was able to show that formations this small would not be safe, but 7 km would be feasible, if challenging. This is what MMS ended up flying in Phase 1b. Similarly, the minimum safe size in Phase 2b was shown to be 20 km: this has become the standard formation size for dayside passes.

3.1 MMS Conjunction Assessment Graphical Outputs

Plots of inter-satellite ranges between the six pairs of MMS spacecraft are a very useful tool for evaluating CAs. In addition, two more sophisticated types of plots are also used for MMS conjunction assessment. These plots, produced by what are known as the MMS Conjunction Assessment Functional Area (CAFA) suite of tools, will now be described. The inputs to both of these tools (and indeed the data that is used to generate ISR plots) are the “restart states”, or state estimates, for the spacecraft that are produced by the MMS GEONS navigation system⁶. This system makes use of GPS signals to determine the MMS orbit: since the bulk of this orbit lies above the GPS constellation, the most complete data is obtained around perigee, when the MMS spacecraft fly through the main lobes of the GPS satellites. The preferred inputs to the CAFA tools are therefore the restart states that are downlinked during a post-perigee communications pass.

3.1.1 Relative Motion Situational Awareness Tool

The Relative Motion Situational Awareness (RMSA) tool is a means of displaying the relative motion between each pair of MMS spacecraft. These states are then propagated out for 10 orbits, with no further maneuvers applied, and the relative motion of the spacecraft plotted in 3-D in terms of a coordinate system centered on one of the spacecraft and with axes along its orbital velocity vector (V), the orbit normal (N), and the binormal direction B that completes the right-handed VNB triad. (For a circular orbit, B would be aligned with the local radius vector; this is generally not the case, however, for the highly eccentric MMS orbit.) The resulting plot is of the type shown in Figure 1; in addition, the mean drift rate per rev is given, as are the minimum ranges on the first and last orbits. This plot helps to provide insight into the possible relative motion between this pair of MMS spacecraft. In particular, since a small difference in the SMA between the two orbits (a common manifestation of maneuver execution errors) predominantly leads to drift along the velocity axis, the N and B motion shown in the RMSA plot tends to be more “robust” than that along V: this helps in understanding how the relative motion will likely evolve over time.

3.1.2 Snapshot Tool

The Snapshot Tool is a platform-independent application which allows the user to view a 3D representation of close approach scenarios. The visual, as Figure 14 depicts, shows a hard-body radius (HBR) sphere around one spacecraft, and a BFMC point cloud of propagated close approach states for the other spacecraft relative to it in the VNB frame of the reference satellite. In the case of MMS, with its 60 meter wire booms, the HBR is taken as 120 m to reflect the extent of both spacecraft combined. The tool gives the probability of collision (Pc), the minimum distance to any of the states (not necessarily the minimum distance for the case with the highest probability of collision), the time of the close approach scenario, and the Pc calculation method (one-to-one [75,000 BFMC cases] or all-to-all [75,000² cases]).

Snapshot plots are produced under two circumstances: the first is when a non-zero probability of collision is computed; the second is when the minimum range falls below some user-defined threshold, e.g. 300 m. If the point cloud associated with this event does not penetrate the HBR, there will be a zero probability of collision, and so the event will not appear on the collision “watch list”. However, situational awareness is improved if the user is aware of such close flybys: they are therefore put onto a separate “events list”, and snapshot plots generated.

3.2 Available Maneuvers for Conjunction Avoidance

The preferred approach to dealing with a predicted conjunction between two MMS spacecraft is to bring forward (i.e., perform early) the next scheduled formation maneuver set. However, in the event that there is insufficient lead time between the detection of the conjunction and the predicted CA, two types of avoidance maneuvers have been designed. Fortunately, neither of these has yet been required to be performed “in anger” to mitigate a CA. One type is the trim burn that has already been discussed; the second is the Dodge maneuver. This was developed before launch as a pre-planned technique for dealing with conjunctions between either two MMS spacecraft or an MMS

and a Resident Space Object (RSO). RSO conjunctions typically occur down near the MMS perigee, as most other spacecraft in intersecting orbits are at altitudes down near the MMS perigee. MMS-to-MMS conjunctions would also typically be expected to occur down in this regime, and in particular at true anomalies in the vicinity of 90 or 270 deg. The reason for this is that conjunctions are most likely to occur where the orbit planes of the two MMSs cross: since optimizing the formation shape for science collection around apogee requires that out-of-plane separation be maximized there, this puts the plane crossings at around 90 and 270 deg. The four MMS orbits are designed to prevent conjunctions by ensuring that there is separation either along-track or radially at the plane crossings: however, a botched burn could lead to an unintended close approach. If this is recognized far enough ahead of time, it could be dealt with by bringing forward a regular FM maneuver set. However, this approach is not feasible if the conjunction is only identified shortly before the Time of Closest Approach: it is for this purpose that the Dodge maneuver was designed.

The Dodge is a single burn by a single spacecraft, one of the CA pair. In some cases, there may be freedom to select which of these two MMSs should dodge; however, for cases where the CA results from a botched burn by one spacecraft, it would presumably not be able to maneuver again so soon, requiring that the other CA spacecraft be the “dodger”. The Dodge Δv (at most 0.5 m/s magnitude) lies in the orbit plane and is designed to shift the position of the maneuvering MMS by the largest amount possible at the CA location, which is taken to be at 270 deg true anomaly. (The 90 deg case gives more time between Dodge and CA, and so is somewhat more benign: a Dodge that gives sufficient separation at 270 deg will do even better at 90 deg.) The original Dodge implementation applied the maneuver at a fixed true anomaly of 200 deg; however, the code was subsequently generalized to allow the Dodge position to be selected arbitrarily, for instance to match available communication contacts. Note that, for the more usual case where there is a considerable time between the maneuver and the conjunction, a burn along the velocity vector would maximize the change in semi-major axis (SMA), and hence period, and hence along-track separation. However, in the “dodgy” case, the relatively short lead time between Dodge and conjunction implies that the separation at the TCA can actually be maximized by burning in a different direction, giving not only a SMA-related along-track shift, but also a “direct” radial shift. The Dodge maneuver achieves the maximal separation possible for a given burn magnitude by optimizing burn direction as a function of the selected burn true anomaly.

MMS has not yet had to carry out a Dodge maneuver, as most conjunctions are identified long enough beforehand to deal with them using a normal FM set or prevented by a trim. However, software is in place to dodge if this ever becomes necessary in the future. In addition, the Maneuver Trade Space (MTS) tool is available for providing insight into when, and with what magnitude, a Dodge burn should be performed for best results.

3.3 Conjunction Assessment Example

Examples of the conjunction assessment plots described above will now be given for an event in Nov. 2016 when MMS3 missed the second burn in an FM pair as a result of the loss of a ground contact. (MMS3 was preempted by higher-priority coverage of a launch.) This left MMS3 on a trajectory quite different from that which was planned, which set it up for a conjunction with MMS2 early the next day: the associated inter-satellite range plot (Figure 12) shows the imminent close approach. Design in parallel of a Dodge and a trim burn was immediately initiated in case it was decided that a maneuver would be required, and a decision meeting was called for later that evening. This meeting was timed to overlap with the arrival of the first set of post-perigee navigation data, which would give the best look at the true orbital state of affairs; the start of the meeting discussed the more preliminary, but available, pre-perigee data.

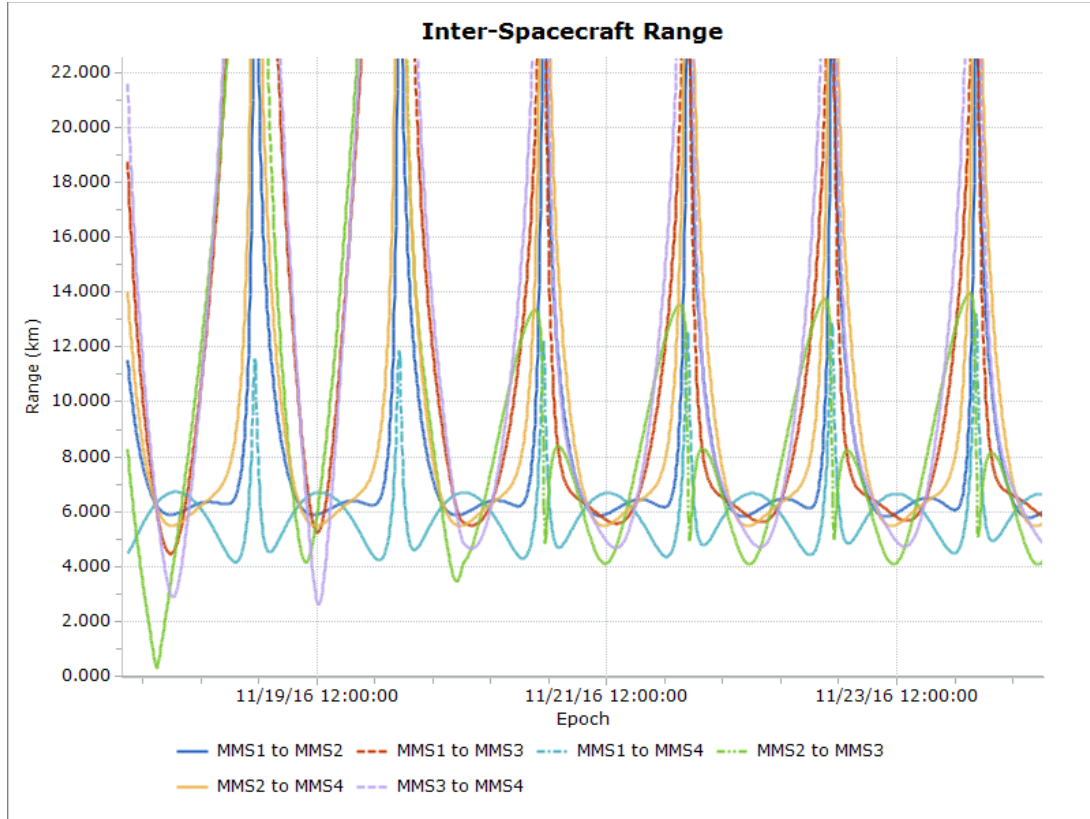


Figure 12. MMS Inter-Satellite Range Plot for Nov. 2016 Missed Burn Case

The pre-perigee data set gave a minimum ISR value of 315 m, which increased to 375 m when examining the post-perigee states: see the RMSA plot of Figure 13. Figure 14 gives the corresponding snapshot plot. Given this improvement in miss distance and the fact that a zero probability of collision was computed by the BFMC tool, the decision taken at the end of the telecon was that a CA mitigation maneuver was not required. Indeed, MMS3 and MMS2 passed by one another tightly but safely. The decision not to maneuver was confirmed the next day by examining the second post-perigee OD solutions: these are the best data available, but were not available until after the decision had to be made.

MMS has taken two actions to avoid any such events in the future. Firstly, MMS maneuvers are now always uploaded to the spacecraft beforehand: loss of a ground contact therefore does not lead to loss of a maneuver. Secondly, when designing a set of formation maneuvers, a thorough screening is carried out of all possible missed burn events, and any formation that would experience close approaches after a missed burn is excluded from consideration. This is quite a severe constraint when designing small tetrahedra, but is definitely judged to be worthwhile in light of the Nov. 2016 event. As a result, no more such events have been experienced since.

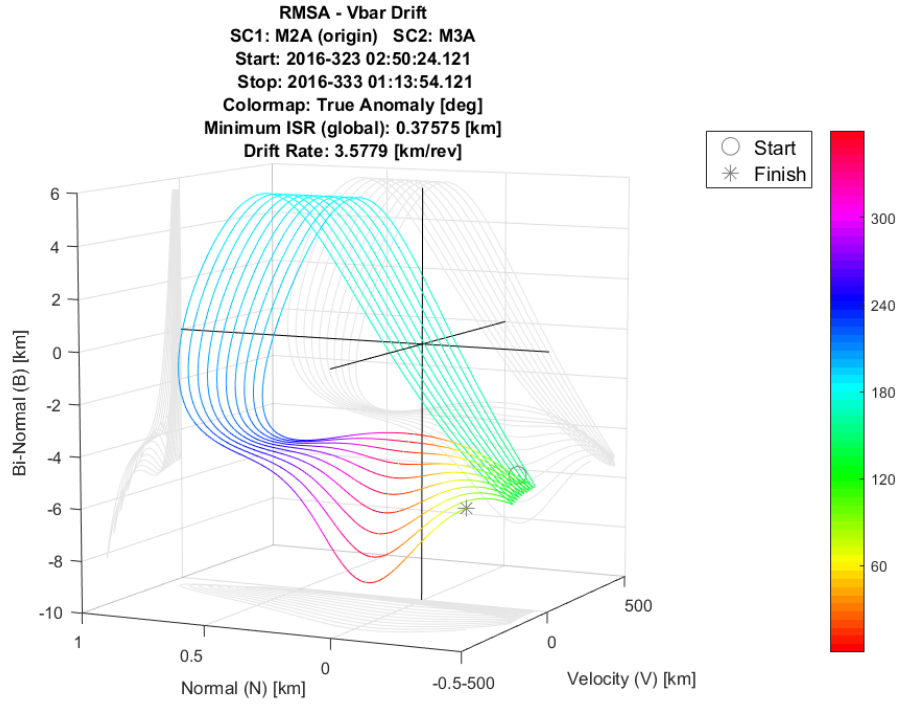


Figure 13. RMSA Plot for Post-Perigee 1 Restart States (color scale indicates TA in degrees)

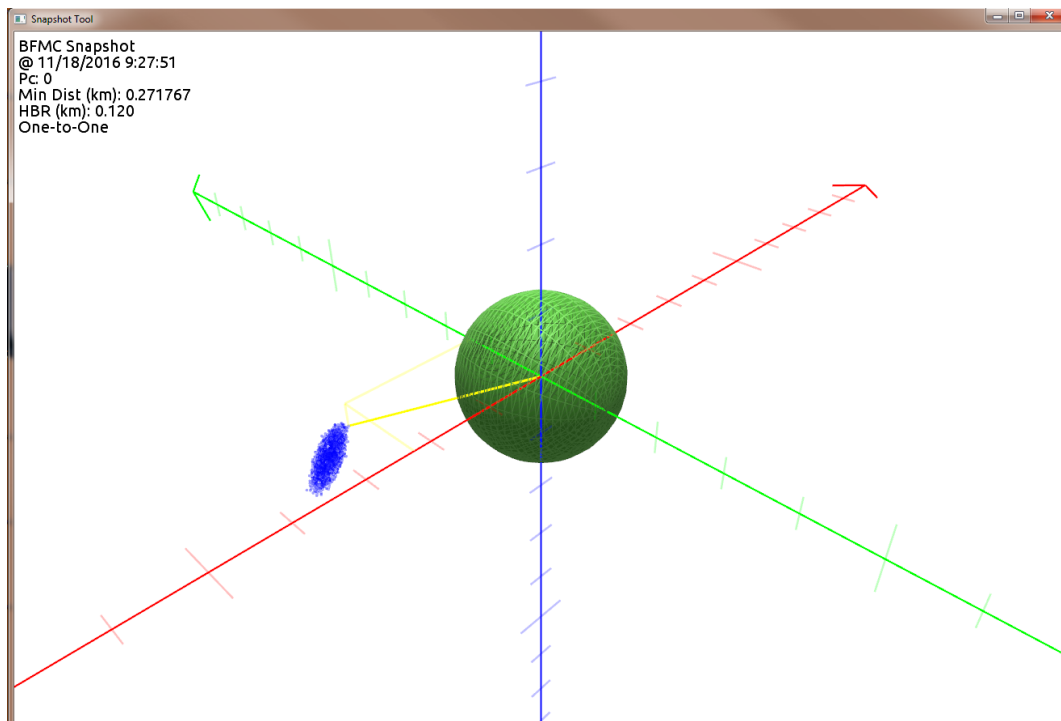


Figure 14. Snapshot Plot for Post-Perigee 1 Restart States (sphere denotes MMS2 HBR, MMS3 solutions form a point cloud)

4. Apogee-Raise Design and Results

The Phase 2a apogee-raise campaign raised apogee radius from the initial 12 R_E required for dayside science to the 25 R_E value required for exploration of the magnetotail. Several features made apogee-raising challenging. Firstly, the MMS thrusters are sized for the small formation maintenance and resize maneuvers that the spacecraft more typically perform: this makes them rather undersized for extensive orbital maneuvering. To be specific, the average dry mass of each spacecraft was 937.9 kg, its initial fuel mass was 411.6 kg, and it is equipped with eight 4 lbf (18 N) radial thrusters (firing in the MMS spin plane), together with four 1 lbf (4.5 N) thrusters aligned with the spacecraft spin axis (two along +Z, two along -Z). The resulting low acceleration implies that apogee-raising cannot be carried out in a single maneuver: this would require burning over an extremely long burn arc, leading to excessive “gravity losses”. Since apogee-raising uses approximately 40% of the total available for the mission, efficiency is important. In addition, the time available for apogee-raising was limited to roughly three months: any more would eat into the limited duration available for reconnection science collection in the magnetotail. (Phase 2b is the single tail passage included in the MMS prime mission.) In order to balance these two considerations, it was decided that each spacecraft should perform a sequence of eight maneuvers.

A further complication is that it was required to be in contact with each spacecraft for at least the start of each maneuver*, and it is only possible to communicate with one MMS at a time. This led to an arrangement where a single spacecraft would burn on nearly each successive perigee. It was also desired that all four spacecraft finish apogee-raising relatively close together, so as not to require excessive fuel to get back into formation. This requires not only that the spacecraft have the same phasing at the completion of the campaign, but that they not become too separated in altitude during the AR sequence: such a separation would be likely to lead to large differential lunisolar perturbations to the orbits.

4.1 Nominal Apogee-Raising “Snake” Design

The scheme that was developed was to break the apogee-raise campaign into four “snakes”, each of which consists of two maneuvers for each spacecraft, or eight in total. These are performed upon successive perigees in the order MMSa MMSb MMSc MMSd MMSd MMSc MMSb MMSa, with a “blank” perigee between the two MMSd burns for orbit determination and replanning of the second burn. In addition, a perigee without maneuvers was inserted after the first and second snakes, to allow additional time to recover from any contingencies that may have occurred.

Each of the eight burns in a snake is targeted to achieve an equal increase in orbital period: this can be seen to lead, in the absence of maneuver execution errors, to the satellites becoming widely separated halfway through the snake, but back in phase at its end. A small modification to the first snake was that “period biasing” was used to spread the spacecraft out somewhat, in order to protect the satellites from conjunctions that could possibly have occurred as a result of the expected effects of maneuver execution errors. This biasing increased the targeted period change of the first burns by 2 min, and reduced the change introduced by the second burns by 2 min. This intentionally alters the rephasing property of the snake, leaving the spacecraft spread by several hundred km at apogee at its completion. Note that this separation is accomplished without the use of either additional fuel or time. By contrast, the original plan to ensure safety from conjunctions had been to increase formation size to 160 km immediately before the start of the apogee-raising campaign: this would have consumed significant additional fuel. Using the period biasing technique allowed this formation resize to be reduced to 60 km, so reducing the amount of fuel required to achieve it.

4.2 Attitude for Apogee-Raising

It was found to be more efficient in terms of fuel to perform the apogee-raise burns using essentially only the radial thrusters, which fire in the spin plane: the axial thrusters were used only for limited attitude control. Also, the 60 m long wire booms of the spinning MMS spacecraft make large slews challenging, so the apogee-raise maneuvers had to be performed in nominal science attitude: spin axis nearly aligned with Ecliptic North but tipped

* The original position was that continuous contact was required throughout all maneuvers. However, after much discussion and analysis, this was revised to requiring contact only at the start of each burn. This has now been relaxed further: the current position is that maneuvers can be carried out when not in contact if necessary.

2-3 degrees towards the Sun. For maneuver efficiency, it was important that the spin plane (in which the thrust was applied) be nearly aligned with the orbit plane (which contained the desired AR DV). A key MMS launch window constraint was therefore that Earth oblateness should cause the orbit normal to precess to relatively close to the Ecliptic normal at the start of the apogee-raising campaign: see the blue near-vertical lines in the launch window plot of Figure 3.

4.3 Apogee-Raise Campaign Flight Results

Table 1 lists the total number of maneuvers (broken into Delta-V [DV] translational and Delta-H [DH] attitude burns) required either to perform apogee-raising, separate the spacecraft for safety before it, or get back into formation afterwards. (The perigee-raise maneuvers that are listed were needed following apogee-raising as a result of the increased perigee variations created by enhanced lunisolar effects in the new higher orbit.) The AR DV burns ranged in magnitude (impulse equivalent) from 24.7 to 48.6 m/s, and each took up to around an hour to perform in an arc around perigee. The entire AR campaign took 92 days. Since apogee-raising consumed about 40% of the original MMS fuel load, the efficiency of the maneuvers was a significant concern, particularly as it had a major impact on how long an extended mission would be feasible. Fortunately, each MMS only consumed approximately 160 kg for apogee-raising, which compared favorably with the originally predicted value of 165 kg.

Table 1. Number of Apogee-Raise-Related Maneuvers

Maneuver Type	Number of DVs	Number of DHs	Total
Formation resize (Phase 1, to 60 km)	6	7	13
Apogee-raise	32	32	64
Perigee-raise	4	4	8
Formation Initialization (Phase 2b 160 km)	6	7	13
<i>Total</i>	<i>48</i>	<i>50</i>	<i>98</i>

A fundamental point concerning the performance of the apogee-raising maneuvers is, of course, the evolution of apogee radius throughout the campaign. Figure 15 displays this for the four spacecraft: it can be seen that the apogee radii of each of the four orbits remain close at the end of each snake. Figure 16 then illustrates the evolution of the six sidelengths between the MMS spacecraft during the campaign. As expected, it can be seen that the satellites spread apart during the first half of each snake, reaching a wide but stable separation after the first four burns. At this point, each spacecraft has the same apogee radius, and hence the same orbital period: the inter-satellite ranges therefore remain fixed until the fifth and subsequent burns are applied. During this second half of the snake the satellites close in again, reaching relatively close spacings at the end of this snake and before the start of the next.

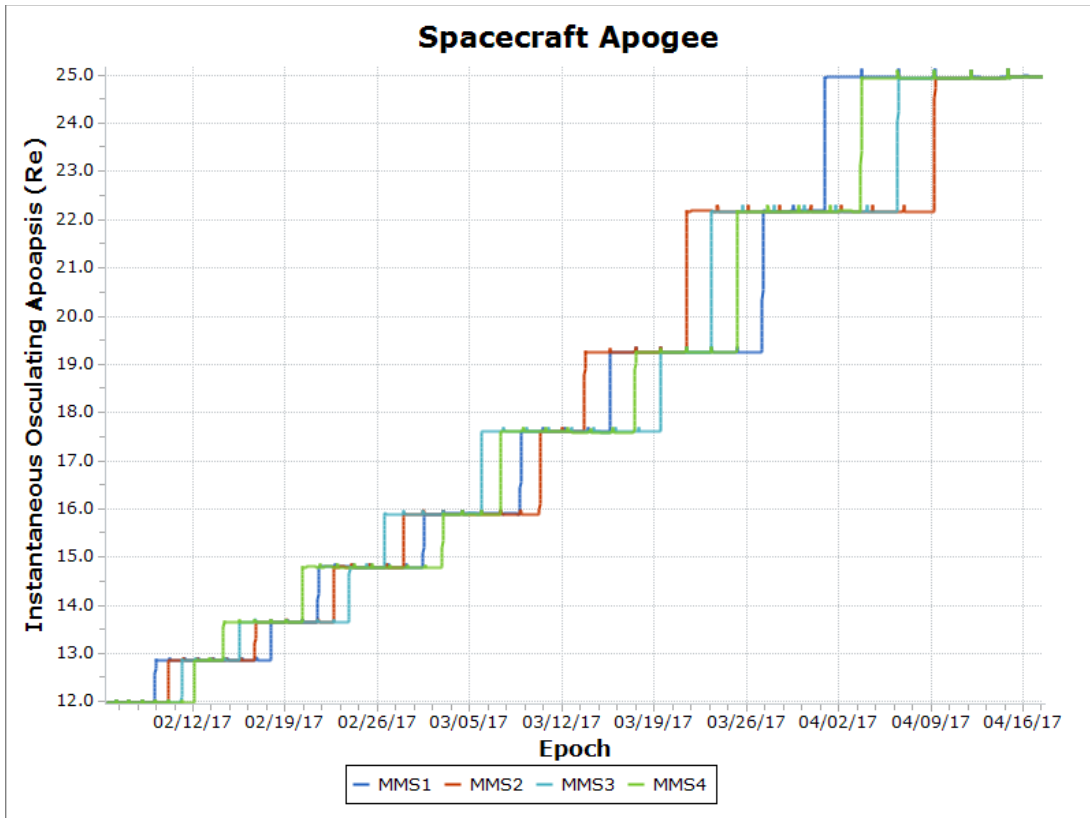


Figure 15. Evolution of Apogee Radii Through AR Campaign

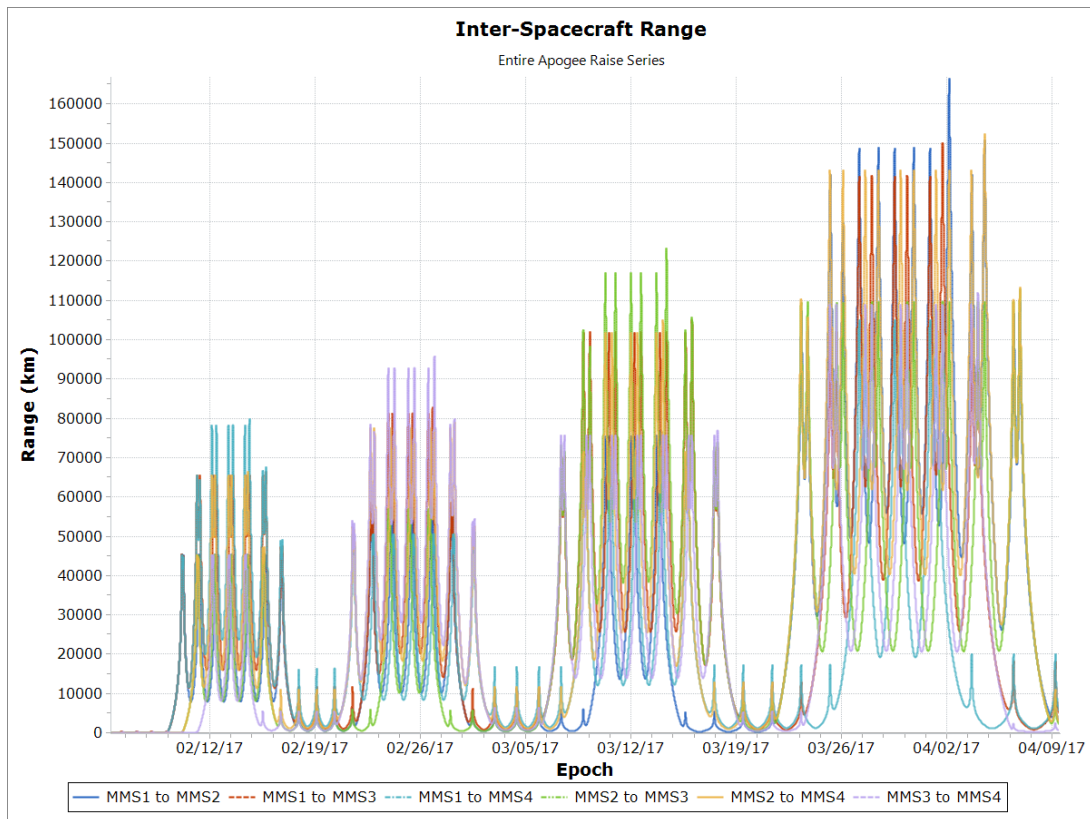


Figure 16. Inter-Satellite Ranges Throughout AR Campaign

The execution errors for all 32 AR burns as determined from navigation data after each maneuver were all very modest: between 0.011% and 0.292% hot. In fact, all but one were in the range 0.011-0.053% hot. These errors are far smaller than the requirements that were imposed on the Delta-V controller, and smaller than was expected prior to apogee-raising: this reduced the dispersions in relative satellite positions that resulted during the apogee-raise campaign. It would therefore actually have been safe to fly the spacecraft somewhat closer than they were during the apogee-raise campaign, with no fear of execution errors inducing conjunctions between MMSs.

5. Flight in String of Pearls Configurations

5.1 Motivation for String Campaign

On April 21, 2023 the MMS Science Working Group approved a proposal for the string campaign from 2024-2025. The campaign intended to cover a year with flight formations in logarithmic strings as opposed to the nominal tetrahedral formation. Maximum spacecraft separations in this configuration were on the order of tens of thousands of kilometers on the orbit flanks. The goal of the campaign was to support new MMS objectives, specifically Kelvin-Helmholtz studies, shock observations, and turbulence in the pristine solar wind and magnetosheath.

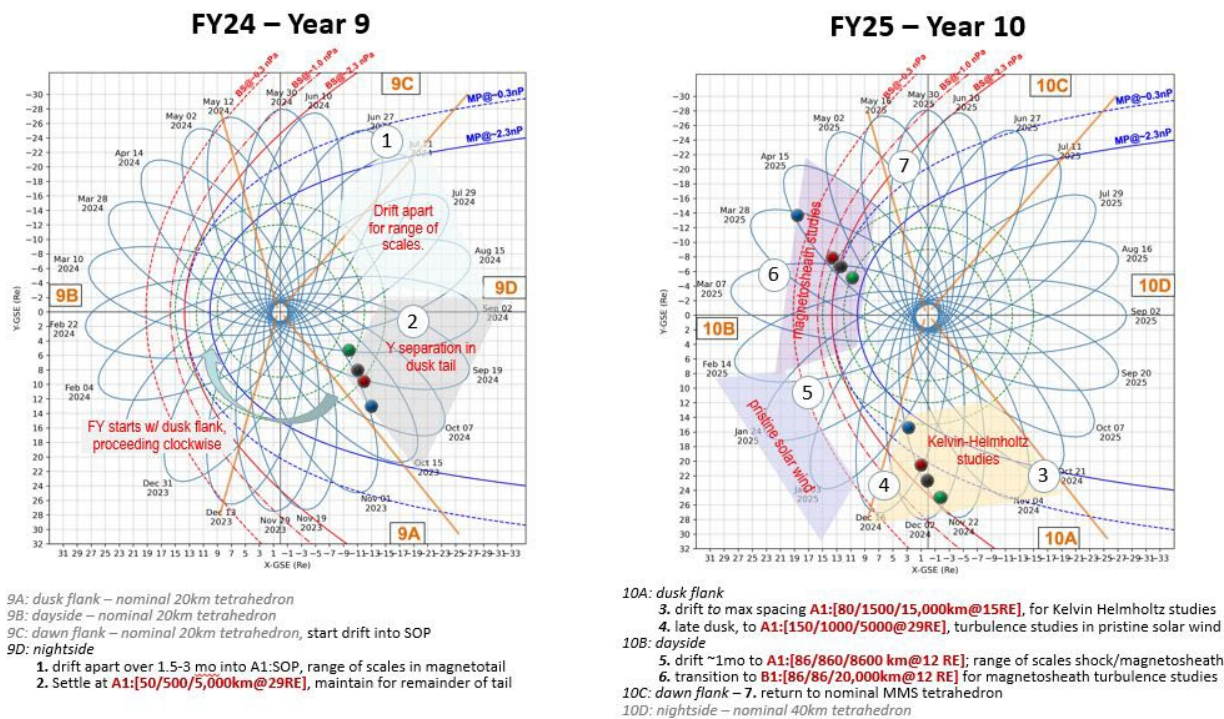


Figure 17. String Campaign Overview

The MMS science team designed the spacecraft separations to expand the scope of the mission’s science objectives. The science team desired gradual drift away from the initial configurations to allow for a continuously varying set of baselines. This approach provided an evolving dataset for analysis, offering scientific insights across a wide region of spacecraft configurations. Toward the end of the campaign, the science team requested a transition of three spacecraft into a triangular formation while positioning the fourth spacecraft at a distant location in a “kite”-like formation. This configuration was designed to capture further scientific data before eventually transitioning back to the nominal tetrahedral formation.

5.2 String of Pearls Maneuver Types

Given that MMS is currently in the extended mission phase with a declining budget, there was no available funding to develop entirely new maneuver design techniques within the software for strings. Therefore, all maneuvers implemented in the string campaign were modifications of existing MMS maneuvers and the FDA was “tricked” into targeting a string formation.

The process of setting up string formations relied primarily on gradual drifting. This method was advantageous for science operations, as it provided evolving baselines, yet also fuel-efficient. The key parameter to maintaining a controlled string formation was to precisely tune the SMA (hence the period) of the four spacecraft. In tetrahedral formations, the SMAs of all spacecraft must be nearly identical to minimize inter-satellite drift and maintain a stable configuration. However, for string formations, the period differences must be set up so as to create desired drift rates, allowing the intended separations to be achieved over time.

The most efficient location for SMA modifications is perigee, so changing apogee radius; in some cases though, this was too efficient as the necessary burn magnitudes at perigee were too small to be accurately executed by the spacecraft. An alternative method was employed by performing a burn at apogee to modify perigee instead. While this approach is less fuel efficient, it allows for better execution accuracy. Throughout the campaign, periodic string maintenance maneuvers were required, especially for the close MMS2/MMS3 pair, to prevent maneuver errors from exceeding specified tolerance limits. This was typically achieved through the use of trim maneuvers.

5.3 Maneuver Results

The string campaign successfully achieved the requested configurations thus far while maintaining fuel efficiency. As seen in Table 2, the total fuel consumption used was approximately 7.2 kg across all four spacecraft so far with an additional 8.42kg expected prior returning to a tetrahedron formation. A total of 8 maneuvers have been executed with a further three to be executed, categorized as follows: 2 FM's, 3 Trims, 3 Apogee Adjustments, 2 Perigee Adjustments, and 1 Apogee Change. Recall that FM burns typically involve pairs of spacecraft, therefore some SMA error columns contain two values. Trim maneuvers were executed selectively based on drift nullification requirements for specific spacecraft. To note, the analysis and discussion presented herein are based on definitive maneuver data up to Feb. 17/18, 2025.

Table 2. String of Pearls Maneuvers

Date	Orbit #	Type	Size (kg)				% Error (delta-SMA)				Purpose
			MMS1	MMS2	MMS3	MMS4	MMS1	MMS2	MMS3	MMS4	
Jun 12/14 2024	1533/1534	Formation Maneuver	1.628		1.058	0.749	1.74%/0.96%		0.67%/1.44%	0.37%/-1.25%	Place in initial string orientation
Jul 5 2024	1539	Apogee Change	0.101	0.091	0.095	0.068	0.27%	1.51%	0.81%	-0.09%	Initiate drift target string
Jul 30 2024	1547	Trim			0.008				3.6%		Adjust MMS3 drift
Sep 16 2024	1560	Apogee Adjust	0.275	0.277	0.269	0.391	0.19%	1.31%	0.34%	-0.79%	Stop MMS4 drift, change MMS1/3 drift to larger spacing with MMS2
Oct 11 2024	1568	Trim		0.006	0.007				-7.15%		Adjust MMS2/3 drift
Nov 14 2024	1578	Trim			0.004				-3.75%		Adjust MMS3 drift
Jan 15 2025	1595	Perigee Adjust	0.892		0.212		-0.15%		-0.54%		MMS1/3 drift to smaller spacing with MMS2
Feb 17/18 2025	1605	Perigee Adjust	0.878		0.189		-0.03%		0.21%		Stop MMS1/3 drift
Mar 6/7 2025	1609/1610	Formation Maneuver	3.727	3.462	0.730						Place MMS1/2/3 into triangle (one side of tetrahedron)
May 1 2025	1626	Apogee Adjust				0.241					Start MMS4 drift towards triangle
Jun 16 2025	1639	Apogee Adjust				0.260					Stop MMS4 drift
Jul 6-8 2025	1644/1645	Formation Maneuver		0.949	0.856	1.222					Return to Tetrahedron (40km)

Provided in Figure 18-Figure 20 are evolutions of the separation distances between spacecraft over time, relative to the reference spacecraft at apogee (MMS2). In Figure 18 for MMS1, the green line represents the definitive or predicted separation, while the red dashed lines indicate the $\pm 25\%$ tolerance boundary. The separation distance gradually increased from approximately 50 km to over 500 km between June and December 2024. A decrease in separation occurred in January 2025, coinciding with the perigee adjust for MMS1 and 3 to drift to a smaller spacing with MMS2. In Figure 19 for MMS3, the general trend is similar to MMS1 with a more controlled increase in separation, peaking at 120 km. The decrease in separation in January 2025 as seen in MMS1 is present, coinciding with the perigee adjust. In Figure 20 for MMS4, separation trends in the negative direction, moving to significantly larger distances compared to MMS1 and MMS3 (up to -4000 km relative to MMS2 at apogee). This indicates MMS4's role as a "sentinel" spacecraft, maintain a large distance from the central formation prior to rejoining the traditional tetrahedral structure later in 2025.

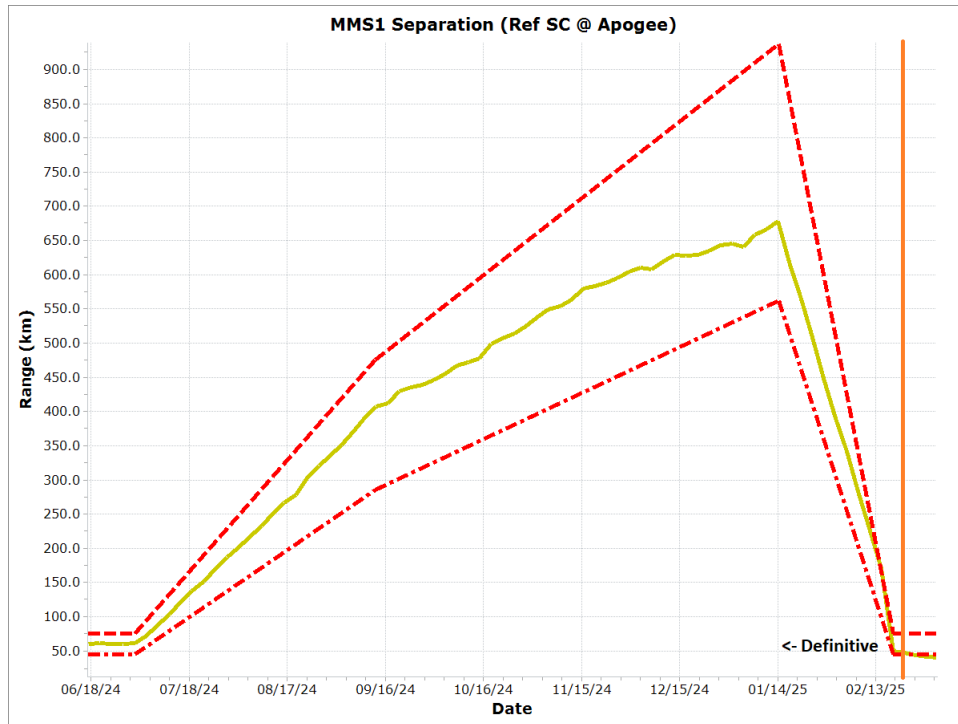


Figure 18. MMS1 Definitive and Predicted Separation for String Campaign

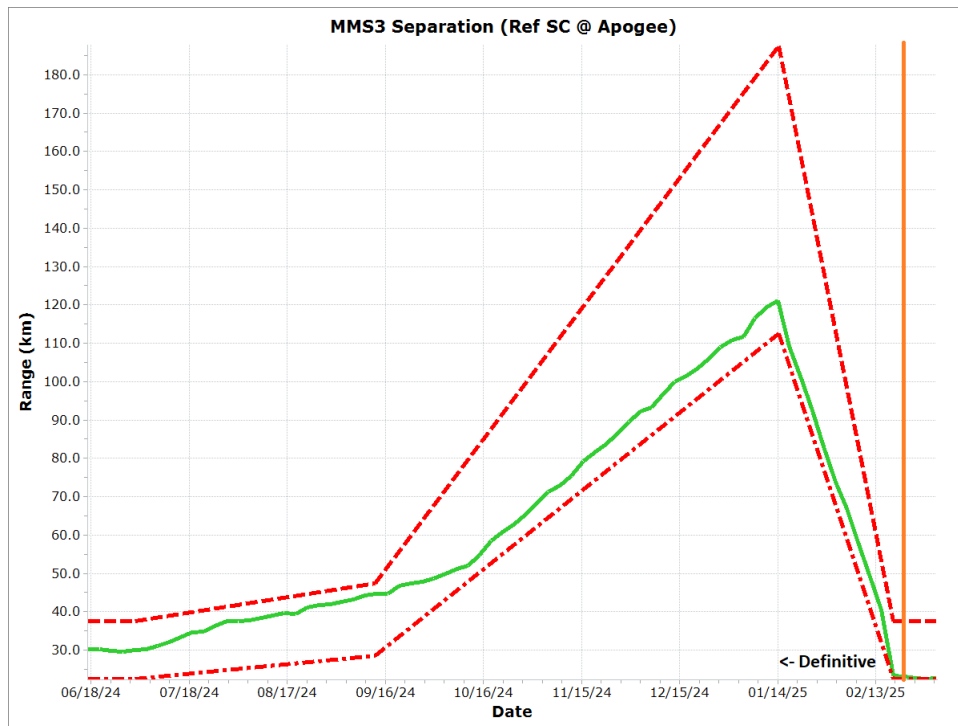


Figure 19. MMS3 Definitive and Predicted Separation for String Campaign

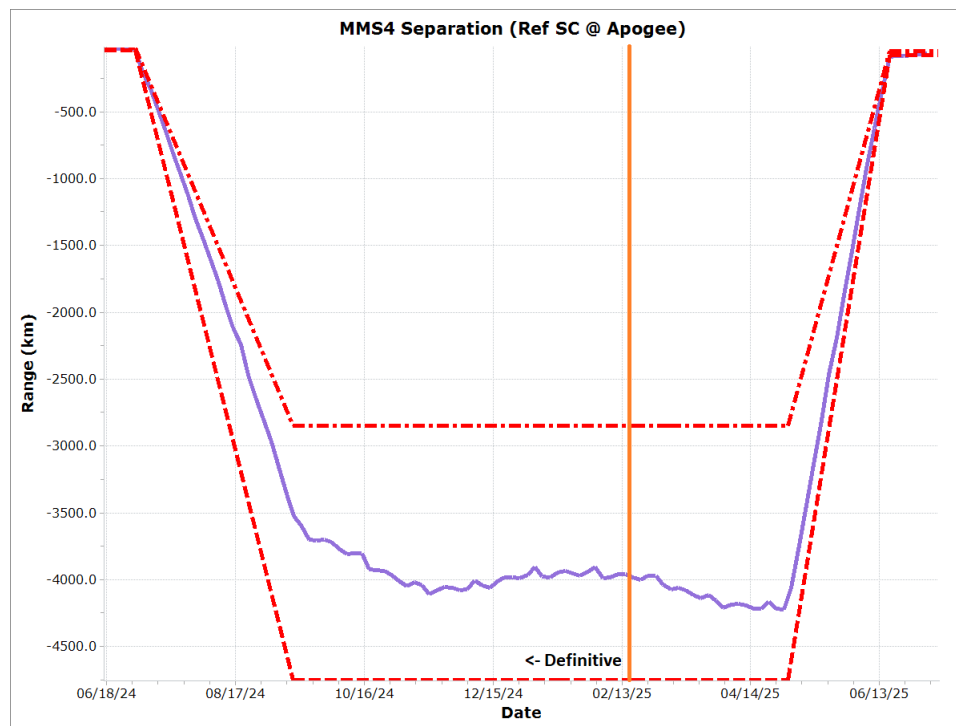


Figure 20. MMS4 Definitive and Predicted Separation for String Campaign

6. Conclusions

This paper has described the underlying dynamics governing formation flying for the MMS mission, the design of maneuvers to accomplish this, and the results obtained during 9 years of flight so far. The results demonstrate that MMS has been able to carry out formation flying while exceeding requirements for maneuver accuracy and cadence. The paper also discussed the other types of maneuvers that the MMS spacecraft have had to perform, many of which were driven by the main source of perturbation to the high MMS orbit (with apogee halfway to lunar orbit), namely the gravitational attractions of Sun and Moon.

Acknowledgements

The authors wish to acknowledge the invaluable contributions of the other members of the MMS Flight Dynamics team, past and present.

References

- [1] A.S. Sharma and S.A. Curtis, "Magnetospheric Multiscale Mission", *Nonequilibrium Phenomena in Plasmas*, Astrophysics and Space Science Library Vol. 321, Springer-Netherlands. pp. 179–195, 2005. DOI 10.1007/1-4020-3109-2_8
- [2] T. Williams, "Launch Window Analysis for the Magnetospheric Multiscale Mission", Paper AAS12-255, AAS/AIAA Space Flight Mechanics Meeting, Charleston, SC, Jan./Feb. 2013. <https://ntrs.nasa.gov/citations/20140010795>
- [3] T. Williams, N. Ottenstein, E. Palmer and M. Farahmand, "Initial Satellite Formation Flight Results from the Magnetospheric Multiscale Mission", Paper AIAA 2016-5505, AIAA SPACE-2016, Long Beach, CA, Sept. 2016. <https://ntrs.nasa.gov/citations/20160010498>
- [4] T. Williams, N. Ottenstein, E. Palmer and D. Godine, "Satellite Formation Flight Results from Phase 1 of the Magnetospheric Multiscale Mission", International Workshop on Satellite Constellations and Formation Flying, Boulder, CO, June 2017. <https://ntrs.nasa.gov/citations/20170005560>
- [5] T. Williams, N. Ottenstein, E. Palmer and J. Hollister, "Results of the Apogee-Raising Campaign of the Magnetospheric Multiscale Mission", Paper AAS 17-760, AAS/AIAA Astrodynamics Specialist Conference, Stevenson, WA, Aug. 2017. <https://ntrs.nasa.gov/citations/20170007741>

- [6] D.H. Fairfield, “A Statistical Determination of the Shape and Position of the Geomagnetic Neutral Sheet”, *J. Geophysical Research*, Vol. 85, No. A2, pp. 775-780, Feb. 1980. DOI 10.1029/JA085iA02p00775
- [7] D.J. Chai, S.Z. Queen and S.J. Placanica, “Precision Closed-Loop Orbital Maneuvering System Design and Performance for the Magnetospheric Multiscale Formation”, Paper 181, 25th International Symposium on Space Flight Dynamics, Munich, Germany, Oct. 2015. <https://ntrs.nasa.gov/citations/20150022197>
- [8] A. Long, M. Farahmand and J.R. Carpenter, “Navigation Operations for the Magnetospheric Multiscale Mission”, Paper 015, 25th International Symposium on Space Flight Dynamics, Munich, Germany, Oct. 2015. <https://ntrs.nasa.gov/citations/20150020825>
- [9] S.P. Hughes, “Formation Design and Sensitivity Analysis for the Magnetospheric Multiscale Mission (MMS)”, Paper AIAA 2008-7357, *Proc. AIAA/AAS Astrodynamics Specialist Conference*, Honolulu, HI, Aug. 2008. DOI: 10.2514/6.2008-7357
- [10] T.W. Williams, J.R. Carpenter, M. Farahmand, N.A. Ottenstein, M. Demoret and D. Godine, “Conjunction Assessment Techniques and Operational Results from the Magnetospheric Multiscale Mission”, 9th International Workshop on Satellite Constellations and Formation Flying, Boulder, CO, June 2017. <https://ntrs.nasa.gov/citations/20170005561>
- [11] I.I. Shevchenko, *The Lidov-Kozai Effect – Applications in Exoplanet Research and Dynamical Astronomy*, Springer, 2017. DOI 10.1007/978-3-319-43522-0
- [12] M.L. Lidov, “Evolution of artificial planetary satellites under the action of gravitational perturbations due to external bodies”, *Artificial Satellites of the Earth*, Vol. 8, pp. 5-45, 1961 (in Russian). DOI 10.2514/3.1983
- [13] Y. Kozai, “Secular perturbations of asteroids with high inclination and eccentricity”, *Astron. J.*, Vol. 67, pp. 591-598, 1962. DOI 10.1086/108790
- [14] T. Williams, E. Palmer, J. Hollister, D. Godine, N. Ottenstein and R. Burns, “Lunisolar Perturbations of High-Eccentricity Orbits such as the Magnetospheric Multiscale Mission”, AAS/AIAA Astrodynamics Specialist Conference, Portland, ME, Aug. 2019. <https://ntrs.nasa.gov/citations/20190029165>
- [15] T. Williams, S. Shulman, N. Ottenstein, E. Palmer, C. Riley, S. Letourneau, J. Hollister, Y. Tedla and D. Godine, “Operational Techniques for Dealing with Long Eclipses during the MMS Extended Mission”, IEEE Aerospace Conference, Big Sky, MT, Mar. 2020. <https://ntrs.nasa.gov/citations/20200001623>